Available online at www.sciencedirect.com

ScienceDirect

IFAC PapersOnline CONFERENCE PAPER ARCHIVE

IFAC PapersOnLine 55-22 (2022) 7–12

The role of closed-loop attitude dynamics in adaptive UAV position control

Salvatore Meraglia * **Marco Lovera** *

* *Dipartimento di Scienze e Tecnologie Aerospaziali, Politecnico di Milano, Via La Masa 34, 20156 Milano, Italy (e-mail:{salvatore.meraglia, marco.lovera}@polimi.it)*

Abstract: This paper presents the design and the stability analysis of an adaptive position controller for Unmanned Aerial Vehicles (UAVs). Considering a hierarchical control scheme, the novelty of this work is the definition of a systematic approach to design a position controller based on Model Reference Adaptive Control (MRAC) theory taking into account not-fast closed-loop attitude dynamics. After having reformulated the problem considering the attitude dynamics as pseudo-actuator, the authors exploit an existing Linear Matrix Inequality (LMI) based hedging framework designed such that the adaptation performance is not affected by the presence of actuator dynamics. Results from simulations and from experiments on a platform designed to replicate the longitudinal motion of quadrotors are provided to illustrate the performance of the proposed control scheme.

1. INTRODUCTION

In recent years, the study of Unmanned Aerial Vehicles (UAVs) has received increasing attention thanks to their wide range of application. In particular, quadrotor UAVs have attracted commercial and research interest thanks to their high level of maneuverability and simple mechanical structure. Various controllers have been proposed to track a predefined trajectory or a path for quadrotors. Fixed-gain linear or nonlinear controllers often serve to address the problem satisfactorily when dealing with nominal operation (see, *e.g.*, Hua et al. (2013) for a comprehensive survey). Specifically, several control systems have been developed based on robust control (Invernizzi et al. (2020)), backstepping (Zuo and Mallikarjunan (2017)), sliding mode controller (Madani and Benallegue (2006)), or hybrid control architecture (Naldi et al. (2017)). In Schoellig and D'Andrea (2009) and Meraglia and Lovera (2021), Iterative Learning Control (ILC) was used to update the reference signal to multirotor systems subject to repetitive disturbances to achieve high-performance tracking. However, repetitive operational conditions and controlled environments are essential for these data-based control algorithms. If more challenging scenarios such as, *e.g.*, actuator degradation and faults, severe external disturbances, and parameter uncertainties have to be considered, then approaches capable of learning whilst operating are needed. Adaptive control is an attractive candidate to face the mentioned disturbances and uncertainties for fault-tolerant or reconfigurable unmanned flight (see, *e.g.*, Lavretsky and Wise (2013)). Model Reference Adaptive Control (MRAC) is the most widely known adaptive control technique and there are many interesting results in the control of multirotors (see Dydek et al. (2013) as an example of numerous references on adaptive multirotor control).

Considering a hierarchical control scheme, the contribution of this work is the design and stability analysis of a position controller based on MRAC theory taking systematically into account non-fast closed-loop attitude dynamics. In fact, actuator dynamics pose a significant obstacle to the design and implementation of standard adaptive controllers (Lavretsky and Wise (2013)). In particular, if the actuator dynamics have sufficiently wide bandwidth, then they can be neglected in the design of MRAC (Gruenwald et al. (2020)). However, if the actuator dynamics do not have sufficiently wide bandwidth or the control system is used for safety-critical applications, a systematic approach must be followed to determine if the actuator bandwidth is large enough to not affect the adaptation performance maintaining the closed-loop dynamical system stable. After having reformulated the problem considering the closed-loop attitude dynamics as pseudo-actuator, the effects of these dynamics on the adaptation performance are analysed exploiting the Linear Matrix Inequality (LMI)-based hedging framework presented in Gruenwald et al. (2016). To the best knowledge of the authors no theoretical analysis of the attitude dynamics effects on the MRAC position controller has been performed so far for a hierarchical control scheme of multirotor UAVs. This paper contributes by evaluating these effects in such an application.

The remainder of this paper is organized as follows. The problem statement is reported in Section 2. In Section 3 we overview the LMI-based hedging MRAC theory. Results from simulation and from experiments on the ANT-X [1] 2DoF drone are provided to illustrate the proposed architecture performance in Section 4 and Section 5, respectively. Finally, concluding remarks are given in Section 6.

Notation: Throughout this paper, $\mathbb{R}(\mathbb{R}_+)$ denotes the set of (positive) real numbers, $\mathbb{R}^n$ denotes the n-dimensional Euclidean space, and $\mathbb{R}^{m\times n}$ the set of $m\times n$ real matrices. Given $A\in\mathbb{R}^{n\times n}$, we use the compact notation $A\in\mathbb{R}^{n\times n}_+$ to represent a positive definite matrix. The i-th vector of the canonical basis in $\mathbb{R}^n$ is denoted as e_i and the identity matrix in $\mathbb{R}^{n\times n}$ is denoted as $I_n := [e_1\cdots e_i\cdots e_n]$. The Euclidean norm of a vector $x\in\mathbb{R}^n$ is $\|x\| := \sqrt{x^\top x}$. The set $\mathrm{SO}(3) := \{R\in\mathbb{R}^{3\times 3} : R^\top R = I_3, \det(R) = 1\}$ denotes the three-dimensional Special Orthogonal group. Given $\omega\in\mathbb{R}^3$, the map $S(\cdot):\mathbb{R}^3\to\mathfrak{so}(3) := \{\Omega\in\mathbb{R}^{3\times 3} : \Omega = -\Omega^\top\}$ is such that $S(\omega)y = \omega\times y$, $\forall y\in\mathbb{R}^3$, where $\times$ represents the cross product in $\mathbb{R}^3$. The inverse of the map S is denoted

[1] ANT-X Website. [Online]. Available: `https://antx.it/`.

10.1016/j.ifacol.2023.03.002

as $S(\cdot)^{-1} : \mathfrak{so}(3) \to \mathbb{R}^3$. This paper interchangeably uses time-domain and frequency-domain representations of signals (*e.g.*, $\psi(t)$ and $\psi(s)$ denote the function of time and its Laplace transform, respectively).

2. PROBLEM STATEMENT

In this section, we first show the dynamical model of vectored-thrust [2] UAV and present a hierarchical control law capable of stabilizing simultaneously the UAV position and heading direction. Then, the interactions between attitude and position loops are analysed. Finally, the UAV model is linearised in near hover conditions to fit the MRAC architecture.

2.1 Mathematical model

The configuration of a rigid UAV can be identified with the motion of a body-fixed frame $F_B := (O_B, \{b_1, b_2, b_3\})$ with respect to a reference frame $F_I := (O_I, \{i_1, i_2, i_3\})$, where b_j and i_j for $j \in \{1,2,3\}$ are unit vectors forming right-handed orthogonal triads and O_B, O_I are the origins of the body and reference frame, respectively. In the following, the position vector from O_I to O_B, resolved in F_I, is denoted as $p = \begin{bmatrix} p_x & p_y & p_z \end{bmatrix}^\top \in \mathbb{R}^3$ while the rotation matrix describing the attitude of the UAV is denoted as $R := \begin{bmatrix} b_1 & b_2 & b_3 \end{bmatrix} \in \mathrm{SO}(3)$, where b_i is the *i-th* body axis resolved in F_I. The dynamical model of a UAV can be described by (Mahony et al. (2012)):

$$\dot{R} = RS(\omega) \qquad J\dot{\omega} = -S(\omega)J\omega + \tau_e + \tau_c \tag{1}$$

$$\dot{p} = v \qquad m\dot{v} = -mgi_3 + T_c R i_3 + f_e, \tag{2}$$

where $J = J^\top \in \mathbb{R}^{3\times3}_+$ is the UAV inertia matrix with respect to O_B, $m \in \mathbb{R}_+$ is the UAV mass, $g = 9.81\,\mathrm{m/s^2}$ is the gravitational acceleration, $\omega \in \mathbb{R}^3$ is the body angular velocity, $v \in \mathbb{R}^3$ is the inertial translational velocity, $T_c \in \mathbb{R}_+$ and $\tau_c \in \mathbb{R}^3$ are the overall thrust and the torque applied by the propellers, respectively, and $(f_e, \tau_e) \in \mathbb{R}^6$ is the disturbance wrench including, *e.g.*, aerodynamic effects and the gyroscopic torque of the rotors.

2.2 Cascade control design for position-yaw stabilization

By relying on the differential flatness property of the dynamics (1)-(2) with respect to the position vector p and to the rotation about the b_3 axis (Formentin and Lovera (2011)), several control strategies have been proposed in the literature to deal with the nonlinear and underactuated nature of the quadrotor dynamics. In this work, the objective of the control design is to stabilize the UAV at a constant position set-point $p^o = \begin{bmatrix} p^o_x & p^o_y & p^o_z \end{bmatrix}^\top \in \mathbb{R}^3$ with a desired yaw angle $\psi^o \in \mathbb{R}$. To tackle the underactuated nature of vectored-thrust UAVs, we follow a hierarchical control strategy in which the attitude dynamics (inner loop) is used to stabilize the translational one (outer loop). Each loop considers the translation and rotation dynamics of the multirotor system separately, hence, reducing the complexity of the control design problem (Roza and Maggiore (2014)).

Position Controller Since the control force in the inertial frame ($T_c R i_3$) cannot be delivered instantaneously in a desired direction, a widely adopted strategy is to introduce a virtual control variable $f_d = \begin{bmatrix} f_{dx} & f_{dy} & f_{dz} \end{bmatrix}^\top$ in equation (2)

$$m\dot{v} = -mgi_3 + f_e + f_d - (f_d - T_c R i_3), \tag{3}$$

where f_d should be selected so that the desired set-point ($p = p^o$, $v = 0$) defines an asymptotically stable equilibrium point of the translational dynamics. In this work, we consider for the altitude stabilization a linear cascade controller as:

$$f_{d_z} := PI_z(s)\left(k^z_p(p^o_z - p_z) - v\right) - D_z(s)v_z + mgi_3\,, \tag{4}$$

where $PI_z(s) := k^{z/i}_p + \frac{k^{z/i}_i}{s}$ and $D_z(s) := k^{z/i}_d \frac{sT^z}{s+T^z}$ are continuous transfer functions defining, respectively, a proportional-integral and (filtered) output-derivative actions , while k^z_p, $k^{z/i}_p$, $k^{z/i}_i$ and $k^{z/i}_d \in \mathbb{R}_+$ are scalar gain and $T^z \in \mathbb{R}_+$ is the filter time constant. Instead, we consider an adaptive controller for the *xy*-plane control (described in the following section) counteracting the unmodelled aerodynamic forces (whose effect in the *z*-axis is considered negligible in this work) to ensure that the UAV tracks a user-specified command with desired transient performance requirements.

Attitude extraction The idea behind the hierarchical approach is to find a reference attitude R_p and a control thrust T_c such that

$$f_d - T_c R_p i_3 = 0. \tag{5}$$

Then, by exploiting the full actuation of the rotational dynamics (1), the control torque τ_c is designed so that the reference attitude R_p is asymptotically tracked. In this way, the mismatch term $f_d - T_c R i_3$ will converge to zero. To solve equation (5), the reference attitude R_p is selected with the third axis aligned with the force required for position stabilization f_d and the rotation about this axis is assigned as a function of a desired yaw angle ($\psi^o \in \mathbb{R}$) through the unit vector $b_{p_1} := \begin{bmatrix} \cos(\psi^o) & \sin(\psi^o) & 0 \end{bmatrix}^\top$, which represents the heading direction. Thus, a solution to equation (5) is $T_c = ||f_d||$ and

$$R_p := \left[\frac{b_{p_3} \times b_{p_1}}{\|b_{p_3} \times b_{p_1}\|} \times b_{p_3} \;\; \frac{b_{p_3} \times b_{p_1}}{\|b_{p_3} \times b_{p_1}\|} \;\; b_{p_3} \right], \quad b_{p_3} := \frac{f_d}{\|f_d\|}\,. \tag{6}$$

Attitude controller In this work we consider the following nonlinear cascade controller for attitude stabilization (similar to the one implemented in the PX4 autopilot [3]):

$$\tau^d_c := PI_R(s)\left(\gamma_R(K^R_p R^\top_d R) - \omega\right) - D_R(s)\omega\,, \tag{7}$$

where $PI_R(s) := K^i_p + K_i\frac{1}{s}$ and $D_R(s) := K_d\frac{sT}{s+T}$ are continuous transfer functions defining, respectively, a proportional-integral and (filtered) output-derivative actions, while K^R_p, K^i_p, K_i and $K_d \in \mathbb{R}^{3\times3}_+$ are diagonal gain matrices and $T \in \mathbb{R}_+$ is the filter time constant. The term $\gamma_R(K^R_p R^\top_d R) := -\frac{1}{2}S^{-1}(K^R_p R^\top_d R - R^\top R_d K^R_p)$ is a nonlinear proportional stabilizer computing the reference angular velocity that must be tracked by the inner loop through a PID controller.

2.3 Interactions between loops

The classical way to design control laws for multirotor UAVs consists in assuming that the controllers will be tuned such that the attitude dynamics would converge faster than translational dynamics. This time-scale separation allows one to neglect the perturbation acting on the translational (outer) loop due to the

[2] Multirotor UAVs with coplanar propellers are known as *vectored-thrust* UAVs, because their propulsive system can deliver a control force only along a fixed direction within the airframe (Hua et al. (2013)).

[3] PX4 community, Dronecode Project, Inc., San Francisco, CA, USA. [Online]. Available: `https://docs.px4.io/en/`.

dynamics of attitude (inner) loop. Namely, if the perturbation term, defined as

$$\sigma = \tfrac{1}{m} T_c (R - R_d) i_3 \ , \tag{8}$$

vanishes rapidly [4] , the complete closed-loop system will be stable in practice Hua et al. (2013). In the literature, different authors quantify how much faster the attitude control loop should be to ensure the closed-loop stability of the whole system (see, *e.g.*, Bertrand et al. (2011) where the stability analysis has been addressed by singular perturbation theory). On the other hand, a hierarchical controller robust to perturbation σ is proposed in Naldi et al. (2017), where the closed-loop stability of the whole system is ensured combining the Input-to-State Stability (ISS) properties of the position error system with the global asymptotic stability of the attitude error subsystem. Similarly, in Invernizzi et al. (2018) the stability of the interconnection between the attitude and position loops is studied within the framework of differential inclusions. Another way to ensure the stability of the whole system is to use standard tools considering the linearised system and to determine when the closed-loop attitude bandwidth (that can be seen as an actuator of the translational dynamics) is too narrow and instability may occur. However, for adaptive control of uncertain dynamical systems, these tools can no longer be used to determine how wide the actuator (closed-loop attitude) bandwidth needs to be to ensure stability. One way to address this issue is to reduce the aggressiveness of the adaptive controller (degrading the tracking performance) by trial-and-error. In contrast, we propose a systematic approach that exploits the hedging-based MRAC architecture (Johnson (2000)) that allows the adaptation performance to not be affected by the presence of actuator dynamics and exploits a LMI-method (Gruenwald et al. (2016)) to determine if the actuator bandwidth is large enough.

2.4 Linearized system

To implement the proposed adaptive architecture, the UAV model in (1)-(2) must be linearised. Assuming near hovering conditions (*i.e.*, $p \approx \bar{p}$, $v \approx 0$, $R \approx I_3 + S(\Delta\alpha)$ with $\Delta\alpha := [\phi \ \theta \ \psi]^\top$ being small rotation angles, $\omega \approx 0$) we obtain:

$$\Delta\dot{\alpha} = \Delta\omega, \qquad \Delta\dot{p} = \Delta v \tag{9}$$

$$J\Delta\dot{\omega} = \Delta\tau_c, \qquad m\Delta\dot{v} = mgS(\Delta\alpha)i_3 + \Delta T_c i_3, \tag{10}$$

where $\Delta T_c := T_c - mg$, $\Delta\tau_c := \tau_c$, and $\Delta(\cdot)$ represent deviation variables. Similarly, the control law can be linearized by recognizing that in near hovering conditions $\|f_d\| \approx mg$ and $\gamma_R(K_p^R R_d^\top R) \approx K_p^R [\phi_d - \phi \ \ \theta_d - \theta \ \ \psi_d - \psi]^\top$, so as to obtain:

$$\Delta T_c := PI_z(s)\left(k_p^z(p_z^o - p_z) - v\right) - D_z(s)v_z, \tag{11}$$

$$\Delta\tau_c := PI_R(s)(K_p^R [\phi_d - \phi \ \ \theta_d - \theta \ \ \psi_d - \psi]^\top - \omega) - D_R(s)\omega, \tag{12}$$

where the desired roll and pitch angles are

$$\phi_d := +\tfrac{1}{mg} f_{d_x} = MRAC(p_y^o, p_y, v_y, \phi), \tag{13}$$

$$\theta_d := -\tfrac{1}{mg} f_{d_y} = MRAC(p_x^o, p_x, v_x, \theta), \tag{14}$$

while ψ_d is the desired yaw angle. In the following, we consider only the dynamics in the xy-plane and focus on the outer-loop controller design with an assumption that a stable inner-loop controller has been applied. The corresponding system state-space form can be written as:

$$\dot{x} = \begin{bmatrix} 0 & 1 & 0 & 0 \\ 0 & 0 & 0 & 0 \\ 0 & 0 & 0 & 1 \\ 0 & 0 & 0 & 0 \end{bmatrix} x + \begin{bmatrix} 0 & 0 \\ -g & 0 \\ 0 & 0 \\ 0 & g \end{bmatrix} w \tag{15}$$

where $x = [p_x \ v_x \ p_y \ v_y]^\top \in \mathbb{R}^4$ $w := [\theta \ \phi]^\top \in \mathbb{R}^2$ is the ouput of the closed-loop attitude dynamics given by

$$w(s) = \begin{bmatrix} G_\theta(s) & 0 \\ 0 & G_\phi(s) \end{bmatrix} u(s) \tag{16}$$

where $u := [\theta_d \ \phi_d]^\top \in \mathbb{R}^2$ is the control input given by the adaptive controller, and $G_\theta(s)$ and $G_\phi(s)$ are the continuous transfer functions defining the closed-loop pitch and roll dynamics respectively. These transfer functions can be either retrieved analytically or identified from experimental data. For the sake of simplicity, in this work $G_\theta(s)$ and $G_\phi(s)$ are approximated by first order dynamical systems [5] . In the following sections we refer to closed-loop attitude dynamics as actuator dynamics.

3. MRAC WITH ACTUATOR DYNAMICS

This section provides a concise overview of Gruenwald et al. (2016) and Gruenwald et al. (2019). In particular, we consider the uncertain dynamical system subject to actuator dynamics

$$\dot{x} = Ax + Bw, \quad x(0) = x_0, \tag{17}$$

where $x \in \mathbb{R}^n$ is the state vector available for feedback, $A \in \mathbb{R}^{n\times n}$ is an unknown system matrix, $B \in \mathbb{R}^{n\times m}$ is a known input matrix, and the pair (A, B) is controllable. $w \in \mathbb{R}^m$ is the actuator output of the actuator dynamics $\mathscr{G}_\mathrm{A}$ given by

$$\begin{aligned} \dot{x}_\mathrm{c} &= -Mx_\mathrm{c} + u, \quad x_\mathrm{c}(0) = x_{\mathrm{c}0}, \\ w &= Mx_\mathrm{c}, \end{aligned} \tag{18}$$

where $x_\mathrm{c} \in \mathbb{R}^m$ is the actuator state vector, $M \in \mathbb{R}_+^{m\times m}$ is a diagonal matrix with diagonal entries representing the actuator bandwidth of each control channel, and $u \in \mathbb{R}^m$ is the control input restricted to the class of admissible controls consisting of measurable functions. Next, we consider the *ideal* reference system capturing a desired closed-loop dynamical system performance given by

$$\dot{x}_\mathrm{i} = A_\mathrm{r} x_\mathrm{i} + B_\mathrm{r} c, \quad x_\mathrm{i}(0) = x_{\mathrm{i}0}, \tag{19}$$

where $x_\mathrm{i} \in \mathbb{R}^n$ is the ideal reference state vector, $c \in \mathbb{R}^m$ is a given uniformly continuous bounded command, $A_\mathrm{r} \in \mathbb{R}^{n\times n}$ is the Hurwitz reference system matrix, and $B_\mathrm{r} \in \mathbb{R}^{n\times m}$ is the command input matrix. We now make the following assumption that is standard in the MRAC literature and is known as the *matching condition* (see Lavretsky and Wise (2013) and Ioannou and Sun (1996)).

Assumption 1. There exist an unknown matrix $W_x \in \mathbb{R}^{m\times n}$ and a known matrix $K_r \in \mathbb{R}^{m\times m}$ such that $A_r = A - BW_x^\top$ and $B_r = BK_r$ hold.

In the presence of actuator dynamics, the standard MRAC formulation based on the (pre-chosen) *ideal* reference model given by equation (19) does not allow the uncertain dynamical system to track the reference model trajectories asymptotically. A remedy to this problem is given by the hedging method (see Johnson (2000) and Johnson and Calise (2003) for more details). This method alters the trajectories of the reference model to allow adaptive controllers to be developed so that

[4] It is assumed that thrust dynamics is negligible with respect to the rigid body dynamics of the UAV, the desired value T_c^d is considered to be instantaneously reached by $T_c = T_c^d$.

[5] The proposed architecture can be easily extended to higher-order dynamics following the approach in Gruenwald et al. (2019).

actuator dynamics have no effect on their stability. Namely, we consider the following *modified* reference model

$$\dot{x}_\mathrm{r} = A_\mathrm{r} x_\mathrm{r} + B_\mathrm{r} c + B[w-u], \quad x_\mathrm{r}(0) = x_{\mathrm{r}0}\ , \tag{20}$$

where the deficit term $B[w-u]$ is introduced. Let the adaptive feedback control law be given by

$$u = -\hat{W}_x^\mathrm{T} x + K_r c\ , \tag{21}$$

where $\hat{W}_x \in \mathbb{R}^{n\times m}$ is the estimate of W_x, which is obtained with the adaptation law

$$\dot{\hat{W}}_x = \gamma \mathrm{Proj}\left[\hat{W}_x, x e^\mathrm{T} P B\right], \quad \hat{W}_x(0) = \hat{W}_{x0}\ , \tag{22}$$

where Proj$[\cdot,\cdot]$ is the projection operator (Lavretsky and Wise (2013)), $\gamma \in \mathbb{R}_+$ being the learning rate, $e \triangleq x - x_\mathrm{r}$ being the system error state vector, and $P \in \mathbb{R}_+^{n\times n}$ being the solution of the Lyapunov equation

$$0 = A_r^T P + P A_r + Q \tag{23}$$

with $Q = Q^\top \in \mathbb{R}_+^{n\times n}$. In addition, the projection bounds are defined such that $\left|\left[\hat{W}_x\right]_{ij}\right| \leq \hat{W}_{x,\max,i+(j-1)n}$ for $i = 1,\ldots,n$ and $j = 1,\ldots,m$, where $\left[\hat{W}_x\right]_{ij}$ denotes the ij-th entry of the matrix $\hat{W}_x$ and $\hat{W}_{x,\max,i+(j-1)n} \in \mathbb{R}_+$ are symmetric [6] element-wise projection bounds.

In Gruenwald et al. (2016), the authors proved that the solutions $\left(e, \hat{W}_x, x_\mathrm{r}, w\right)$ of the closed-loop dynamical system are bounded and $\lim_{t\to\infty} e = 0$ if the following condition is satisfied.

Assumption 2. Let $\bar{W}_{x_{i_1,\ldots,i_l}} \in \mathbb{R}^{n\times m}$ be defined as where $i_l \in \{1,2\}$, $l \in \{1,\ldots,mn\}$, such that $\bar{W}_{x_{i_1,\ldots,i_l}}$ represents the corners of the hypercube defining the maximum variation of $\hat{W}_x(t)$ ensured by the projection operator. The matrix

$$\mathscr{A}_{i_1,\ldots,i_l} = \begin{bmatrix} A_r + B\bar{W}^\mathrm{T}_{x_{i_1,\ldots,i_l}} & BM \\ -\bar{W}^\mathrm{T}_{x_{i_1,\ldots,i_l}} & -M \end{bmatrix} \tag{24}$$

satisfies the matrix inequality

$$\mathscr{A}^\mathrm{T}_{i_1,\ldots,i_l}\mathscr{P} + \mathscr{P}\mathscr{A}_{i_1,\ldots,i_l} < 0, \quad \mathscr{P} = \mathscr{P}^\mathrm{T} > 0, \tag{25}$$

for all permutations of $\bar{W}_{x_{i_1,\ldots,i_l}}$.

Remark 3. Since Assumption 2 is satisfied for large values of M (see Gruenwald et al. (2016)), we can cast (25) as a convex optimisation problem whose solution M is the minimum actuator bandwidth that satisfies Assumption 2 for the given level of system uncertainty. From a practical standpoint, there should be a basic tradeoff between the permitted system uncertainties and the actuator dynamics, as remarked in Gruenwald et al. (2019).

4. ADAPTIVE UAV POSITION CONTROL

In this section, we compare in simulation the proposed control architecture (with hedged reference model) with the standard MRAC. The task is to track a stair sequence in the xy-plane mantaining $\psi_d = 0$. In particular, we use a high-fidelity simulator of quadrotor dynamics in which the altitude and attitude controllers are the ones described in Section 2.2 (which behave for small errors as Section 2.4). The UAV mass is $m = 0.250\,\mathrm{kg}$ and the attitude loops are tuned such that their closed-loop dynamics can be well approximated by first-order systems with $M_\phi = 9\,\mathrm{rad/s}$ and $M_\theta = 5.5\,\mathrm{rad/s}$ as roll and pitch bandwidth, respectively. Furthermore, we consider the body-drag force using the simplified model $f_e := -c_D\|v\|v$ with $c_D = 0.1$ being the body drag coefficient. The adaptive controller synthesis has been carried out by using the linear system (15) with zero initial conditions designing independently the $x-$ and $y-$axis. For both the standard MRAC and the hedged-one, we set $Q = I_2$ from (23) and select a second-order reference system with zero initial conditions, a natural frequency of $\omega_\mathrm{n} = 4\,\mathrm{rad/s}$, and a damping ratio $\zeta = 0.7$. Using the rectangular projection operator, the bounds on the uncertainty (considered equal for the $x-$ and $y-$axis) are set element-wise such that $|\left[\hat{W}_x\right]_{1,1}| < \omega_n^2/g \leq 1.8$ and $|\left[\hat{W}_x\right]_{2,1}| < 2\zeta\omega_n/g \leq 0.65$. Using these bounds and considering the system dynamics (15), we ensure that the uncertain parameters belong to the convex set delimited by the projection operator centered on the origin. Then, using the projection bounds in the LMI optimization problem highlighted in Remark 3, the minimum allowable actuator bandwidth is computed as $M^{\min}_{(\cdot)} = 5.5\,\mathrm{rad/s}$. The adaptation rate is selected as $\gamma_H = 300$ for the proposed architecture and as $\gamma_M = 100$ for the standard MRAC. This choice is dictated by the fact that using a larger adaptation rate $\gamma_M > 100$ for the standard MRAC architecture leads to instability. Figure 1 and Figure 2 show the results obtained with the standard MRAC controller in the presence of fast (roll dynamics) and not-fast (pitch dynamics). We can notice that, especially in x-direction (with not-fast pitch dynamics), the standard MRAC controller introduces unwanted oscillations and deteriorates the tracking performance. On the other hand, Figure 3 and Figure 4 show the performance of the proposed adaptive architecture. After the learning transient, the system response becomes almost identical to the *modified* reference one. Finally, we define the following metric to

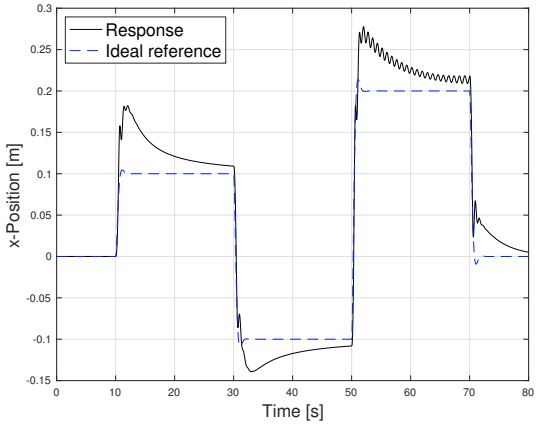

Fig. 1. Standard MRAC performance in x-direction.

compare the performance achieved by the two controllers:

$$e^P(t) := \sqrt{(p_x(t) - p_x^i(t))^2 + (p_y(t) - p_y^i(t))^2}\ , \tag{26}$$

where $p_x^i(t)$ and $p_y^i(t)$ are the x- and y-position given by the *ideal* reference system, respectively. We report in Table 1 the peak ($e^P_{PK} = \max_t e^P(t)$) and the root mean square (e^P_{RMS}) of the signal $e^P(t)$. We can state that the proposed architecture is very

Table 1. Simulation results: performance metrics.

	Hedging-based	Standard MRAC
Peak e^P_{PK} [m]	0.0805	0.1110
RMS e^P_{RMS} [m]	0.0136	0.0314

effective in improving the UAV tracking performance providing

[6] Note that the results of this section can be extended to the case when asymmetric projection bounds are considered, as in Gruenwald et al. (2020).

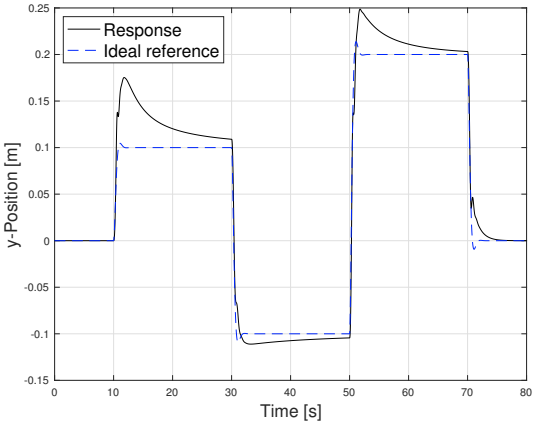

Fig. 2. Standard MRAC performance in y-direction.

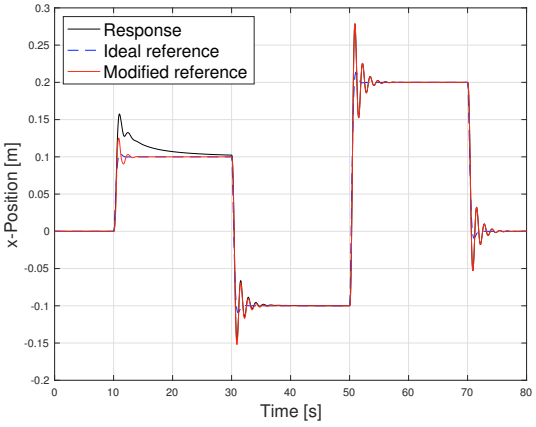

Fig. 3. Proposed architecture performance in x-direction.

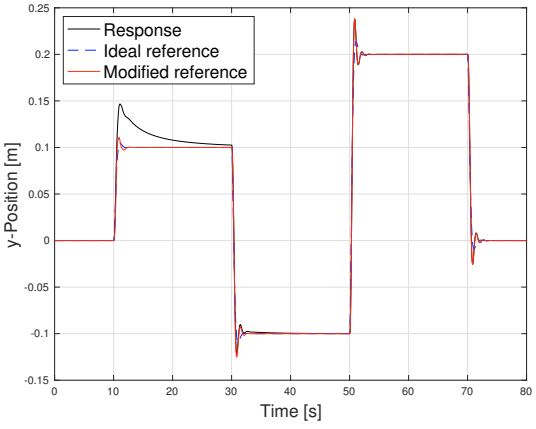

Fig. 4. Proposed architecture performance in y-direction.

a systematic way to take into account the closed-loop attitude dynamics.

5. EXPERIMENTAL RESULTS

The experimental tests performed on the ANT-X 2DoF drone are presented and discussed in this section. The tests are intended to show and compare the behavior of the proposed control architecture with the standard MRAC scheme in a realistic scenario. The ANT-X 2DoF drone setup consists of a small quadrotor UAV constrained to operate along two linear guides, allowing only pitch rotation and longitudinal motion (see Panza et al. (2021) for more details). It has been designed to replicate the longitudinal motion of quadrotors, which is described by the following equations:

$$\dot{\theta} = q, \qquad J_\theta \dot{q} = M_{c_x} + M_{e_x} \tag{27}$$

$$\dot{p_x} = v_x, \qquad m\dot{v}_x = -T_c \sin\theta + f_{e_x} \tag{28}$$

where $\theta,\ q \in \mathbb{R}$ are the pitch angle and rate, respectively, $p_x,\ v_x \in \mathbb{R}$ are the position and velocity along the x-axis, respectively, $m \in \mathbb{R}_+$ is the quadrotor mass, $J_\theta \in \mathbb{R}_+$ is the pitch inertia moment, $T_c \in \mathbb{R}_+$ is the control thrust (imposed constant during the experiments $T_c = mg$), $\tau_{c_x} \in \mathbb{R}$ is the control torque, while $M_{e_x},\ f_{e_x} \in \mathbb{R}$ are torque and force disturbances along the x-axis. Being able to study the longitudinal dynamics is important since it captures all the most relevant challenges associated with the underactuated nature of co-planar multirotors. The task of the experimental campaign is to track a stair sequence in the x-direction. To implement the proposed adaptive architecture the model (27)-(28) is linearised assuming small rotation angle ($\sin\theta \approx \theta$). Similarly to the previous section, for both the standard MRAC and the hedged-one, we set $Q = I_2$ from (23) and select a second-order reference system with zero initial conditions, a natural frequency of $\omega_n = 2.3\,\mathrm{rad/s}$, and a damping ratio $\zeta = 0.7$. Using the rectangular projection operator, the bounds on the uncertainty are set element-wise such that $|\left[\hat{W}_x\right]_{1,1}| < \omega_n^2/g \leq 0.55$ and $|\left[\hat{W}_x\right]_{2,1}| < 2\zeta\omega_n/g \leq 0.35$. Then, using the bounds on $\hat{W}_x$ in the LMI optimization problem, the minimum allowable pitch closed-loop bandwidth is computed as $M_\theta^{\min} = 2.9\,\mathrm{rad/s}$. The attitude loop is tuned such that the closed-loop pitch dynamics can be well approximated by a first-order system with $M_\theta = 3\,\mathrm{rad/s}$ as bandwidth that is close to the allowable limit $M_\theta^{\min}$. Figure 5 and Figure 6 show the position response of the standard MRAC architecture and of the proposed one using $\gamma_H = \gamma_M = 100$. Similarly to the

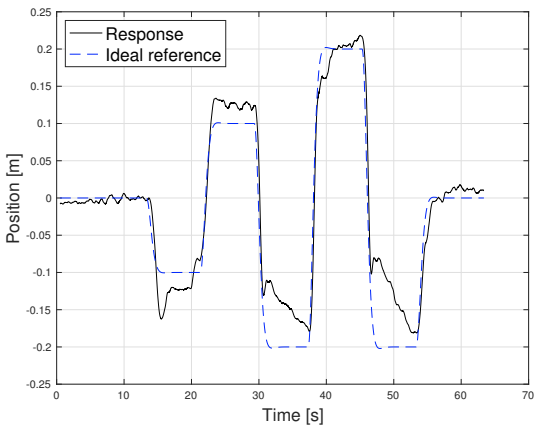

Fig. 5. Drone position with the standard MRAC architecture.

previous section, we define the following metric to compare the performance achieved by the two controllers:

$$e^x(t) := |(p_x(t) - p_x^i(t))|\,. \tag{29}$$

where $p_x^i(t)$ is the x-position given by the *ideal* reference system. We report in Table 2 the peak ($e^x_{PK} = \max_t e^x(t)$) and the root mean square (e^x_{RMS}) of the signal $e^x(t)$. A remarkable performance improvement is obtained with the proposed approach. Furthermore, the LMI-based feasible limit $M_\theta^{\min}$ provides a

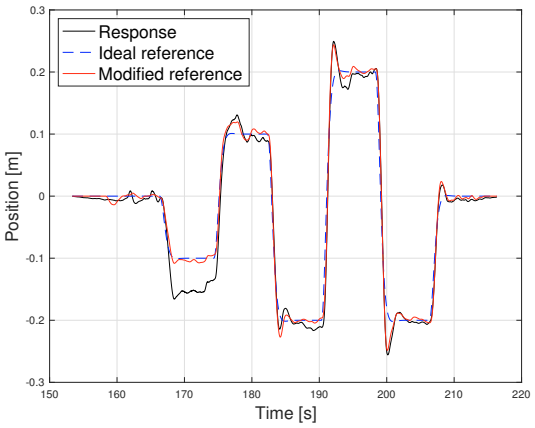

Fig. 6. Drone position with the proposed architecture.

Table 2. Experiment performance metrics.

	Hedging-based	Standard MRAC
Peak e^x_{PK} [m]	0.0860	0.1211
RMS e^x_{RMS} [m]	0.0275	0.0428

(conservative) lower bound on the allowable closed-loop attitude bandwidth such that the overall closed-loop system remains bounded, avoiding trial-and-error tuning procedure.

6. CONCLUSION

In this paper, we defined a systematic approach to design a position controller based on MRAC theory for a quadrotor UAV taking into account the closed-loop attitude dynamics. In particular, after having reformulated the problem considering attitude dynamics as an actuator for the translational dynamics, we exploited the LMI-based hedging MRAC controller (initially proposed in Gruenwald et al. (2016)) to achieve desirable tracking performance specifications despite uncertainties. Finally, results from simulation and experiments on the ANT-X 2DoF drone showed the effectiveness of the proposed strategy.

REFERENCES

Bertrand, S., Gunard, N., Hamel, T., Piet-Lahanier, H., and Eck, L. (2011). A hierarchical controller for miniature VTOL UAVs: Design and stability analysis using singular perturbation theory. *Control Engineering Practice*, 19(10), 1099–1108. doi:https://doi.org/10.1016/j.conengprac.2011.05.008.

Dydek, Z.T., Annaswamy, A.M., and Lavretsky, E. (2013). Adaptive control of quadrotor UAVs: A design trade study with flight evaluations. *IEEE Transactions on Control Systems Technology*, 21(4), 1400–1406. doi: 10.1109/TCST.2012.2200104.

Formentin, S. and Lovera, M. (2011). Flatness-based control of a quadrotor helicopter via feedforward linearization. In *2011 50th IEEE Conference on Decision and Control and European Control Conference*, 6171–6176. doi: 10.1109/CDC.2011.6160828.

Gruenwald, B.C., Yucelen, T., Dogan, K.M., and Muse, J.A. (2020). Expanded reference models for adaptive control of uncertain systems with actuator dynamics. *Journal of Guidance, Control, and Dynamics*, 43(3), 475–489.

Gruenwald, B.C., Yucelen, T., Muse, J.A., and Wagner, D. (2019). Computing stability limits for adaptive control laws with high-order actuator dynamics. *Automatica*, 101, 409–416. doi:https://doi.org/10.1016/j.automatica.2018.12.025.

Gruenwald, B.C., Wagner, D., Yucelen, T., and Muse, J.A. (2016). Computing actuator bandwidth limits for model reference adaptive control. *International Journal of Control*, 89(12), 2434–2452. doi:10.1080/00207179.2016.1161236.

Hua, M.H., Hamel, T., Morin, P., and Samson, C. (2013). Introduction to feedback control of underactuated VTOL vehicles: A review of basic control design ideas and principles. *IEEE Control Systems Magazine*, 33(1), 61–75. doi: 10.1109/MCS.2012.2225931.

Invernizzi, D., Lovera, M., and Zaccarian, L. (2018). Geometric tracking control of underactuated VTOL UAVs. In *American Control Conference*. Milwaukee (WI), USA.

Invernizzi, D., Panza, S., and Lovera, M. (2020). Robust tuning of geometric attitude controllers for multirotor unmanned aerial vehicles. *Journal of Guidance, Control, and Dynamics*, 43(7), 1332–1343. doi:10.2514/1.G004457.

Ioannou, P.A. and Sun, J. (1996). *Robust adaptive control*. Upper Saddle River, NJ: Prentice-Hall.

Johnson, E.N. and Calise, A.J. (2003). Limited authority adaptive flight control for reusable launch vehicles. *Journal of Guidance, Control, and Dynamics*, 26(6), 906–913. doi: 10.2514/2.6934.

Johnson, E.N. (2000). *Limited authority adaptive flight control*. School of Aerospace Engineering, Georgia Institute of Technology. Georgia Institute of Technology.

Lavretsky, E. and Wise, K.A. (2013). *Robust and adaptive control with aerospace applications*. Springer London.

Madani, T. and Benallegue, A. (2006). Backstepping sliding mode control applied to a miniature quadrotor flying robot. In *IECON 2006 - 32nd Annual Conference on IEEE Industrial Electronics*, 700–705. doi: 10.1109/IECON.2006.347236.

Mahony, R., Kumar, V., and Corke, P. (2012). Multirotor aerial vehicles: Modeling, estimation and control of quadrotor. *IEEE Robotics & Automation Magazine*, 19(3), 20–32.

Meraglia, S. and Lovera, M. (2021). Smoother-Based Iterative Learning Control for UAV Trajectory Tracking. *IEEE Control Systems Letters*, 6, 1501–1506.

Naldi, R., Furci, M., Sanfelice, R.G., and Marconi, L. (2017). Robust global trajectory tracking for underactuated VTOL aerial vehicles using inner-outer loop control paradigms. *IEEE Transactions on Automatic Control*, 62(1), 97–112. doi:10.1109/TAC.2016.2557967.

Panza, S., Invernizzi, D., Giurato, M., and Lovera, M. (2021). Design and characterization of the 2DoF drone: a multirotor platform for education and research. *IFAC-PapersOnLine*, 54(12), 32–37. doi: https://doi.org/10.1016/j.ifacol.2021.11.006.

Roza, A. and Maggiore, M. (2014). A class of position controllers for underactuated VTOL vehicles. *IEEE Transactions on Automatic Control*, 59(9), 2580–2585. doi: 10.1109/TAC.2014.2308609.

Schoellig, A. and D'Andrea, R. (2009). Optimization-based Iterative Learning Control for trajectory tracking. In *2009 European Control Conference (ECC)*, 1505–1510. doi: 10.23919/ECC.2009.7074619.

Zuo, Z. and Mallikarjunan, S. (2017). $\mathscr{L}_1$ adaptive backstepping for robust trajectory tracking of UAVs. *IEEE Transactions on Industrial Electronics*, 64(4), 2944–2954. doi: 10.1109/TIE.2016.2632682.